# Periodic production of retinoic acid by meiotic and somatic cells coordinates four transitions in mouse spermatogenesis

Tsutomu Endo[a,1,2], Elizaveta Freinkman[a,3], Dirk G. de Rooij[a], and David C. Page[a,b,c,1]

[a]Whitehead Institute, Cambridge, MA 02142; [b]Department of Biology, Massachusetts Institute of Technology, Cambridge, MA 02139; and [c]Howard Hughes Medical Institute, Whitehead Institute, Cambridge, MA 02142

Contributed by David C. Page, October 4, 2017 (sent for review June 22, 2017; reviewed by Marvin L. Meistrich and Kyle E. Orwig)

**Mammalian spermatogenesis is an elaborately organized differentiation process, starting with diploid spermatogonia, which include germ-line stem cells, and ending with haploid spermatozoa. The process involves four pivotal transitions occurring in physical proximity: spermatogonial differentiation, meiotic initiation, initiation of spermatid elongation, and release of spermatozoa. We report how the four transitions are coordinated in mice. Two premeiotic transitions, spermatogonial differentiation and meiotic initiation, were known to be coregulated by an extrinsic signal, retinoic acid (RA). Our chemical manipulations of RA levels in mouse testes now reveal that RA also regulates the two postmeiotic transitions: initiation of spermatid elongation and spermatozoa release. We measured RA concentrations and found that they changed periodically, as also reflected in the expression patterns of an RA-responsive gene, STRA8; RA levels were low before the four transitions, increased when the transitions occurred, and remained elevated thereafter. We found that pachytene spermatocytes, which express an RA-synthesizing enzyme, *Aldh1a2*, contribute directly and significantly to RA production in testes. Indeed, chemical and genetic depletion of pachytene spermatocytes revealed that RA from pachytene spermatocytes was required for the two postmeiotic transitions, but not for the two premeiotic transitions. We conclude that the premeiotic transitions are coordinated by RA from Sertoli (somatic) cells. Once germ cells enter meiosis, pachytene spermatocytes produce RA to coordinate the two postmeiotic transitions. In combination, these elements underpin the spatiotemporal coordination of spermatogenesis and ensure its prodigious output in adult males.**

retinoic acid | spermatogenesis | mouse | testis

Mammalian spermatogenesis is a choreographed process in which diploid spermatogonia undergo differentiation to give rise to specialized haploid gametes, called spermatozoa. Within the testis, several key developmental transitions of spermatogenesis occur in close physical and temporal proximity. These transitions must be carefully regulated to ensure that large numbers of spermatozoa are produced continuously throughout reproductive life. We address the question of how these transitions are coordinated at the cellular and molecular level.

During spermatogenesis, four key transitions stand out: (*i*) differentiation of spermatogonia, (*ii*) meiotic initiation, (*iii*) initiation of spermatid elongation, and (*iv*) release of spermatozoa into the lumen of seminiferous tubules (Fig. 1). In mice, spermatogenesis begins with undifferentiated type A spermatogonia, which include the stem cells (1–4). Undifferentiated spermatogonia periodically undergo spermatogonial differentiation (also known as the $A_{aligned}$-to-$A_1$ transition) to become differentiating spermatogonia (also known as $A_1$/$A_2$/$A_3$/$A_4$/intermediate/B spermatogonia). During spermatogonial differentiation, the spermatogonia lose the capacity for self-renewal (5) and begin a series of six transit-amplifying mitotic divisions (6). Germ cells then become spermatocytes and undergo meiotic initiation (7, 8). DNA replication and two cell divisions follow, resulting in the formation of haploid, round spermatids, which elongate their nuclear and cytoplasmic contours to become spermatozoa. Finally, these spermatozoa are released into the lumen of seminiferous tubules.

The four key transitions of spermatogenesis are precisely coordinated in time and space and occur in close physical and temporal proximity, cyclically, with an 8.6-d periodicity in mice (9). The mouse testis is composed of structures known as seminiferous tubules (Fig. S1*A*); within tubule cross-sections, one sees stereotypical collections or associations of germ cells at various steps of differentiation (Fig. 1). The precise coordination of these steps is called the "cycle of the seminiferous epithelium" (or "seminiferous cycle"). In mice, researchers have characterized 12 distinct cellular associations, known as seminiferous stages I to XII (10); the four key transitions all occur in stages VII and VIII (10, 11) (Fig. 1 and Fig. S1 *B–D*). This intimate proximity of the four transitions to each other is largely conserved in other mammals, including humans (12), rats (13, 14), hamsters (15), and rams (15). The layered generations of germ cells in the seminiferous tubule are embedded in and supported by somatic (Sertoli) cells that supply factors essential for spermatogenesis (16). We sought to investigate the cooccurrence of the four key transitions, to understand the regulation of these transitions and the overall organization of spermatogenesis.

Both of the premeiotic transitions—spermatogonial differentiation and meiotic initiation—require retinoic acid (RA), a derivative

## Significance

**Male mouse sex cells mature into sperm through a 35-d process punctuated by four transitions, two occurring before meiosis (spermatogonial differentiation and meiotic initiation) and two after meiosis (spermatid elongation and sperm release). The four transitions occur in proximity spatially and temporally, with an 8.6-d periodicity. We describe how this coordination is achieved. The premeiotic transitions were known to be regulated by retinoic acid (RA). We show that RA also regulates the two postmeiotic transitions. RA levels change periodically, and meiotic cells contribute to its production. The two postmeiotic transitions require RA from meiotic cells while the premeiotic transitions require RA from somatic cells. These elements underpin the spatiotemporal coordination of spermatogenesis to ensure constant sperm production throughout adult life.**

Author contributions: T.E., D.G.d.R., and D.C.P. designed research; T.E. and E.F. performed research; T.E., E.F., and D.G.d.R. analyzed data; and T.E. and D.C.P. wrote the paper.

Reviewers: M.L.M., MD Anderson Cancer Center; and K.E.O., Magee-Womens Research Institute.

Conflict of interest statement: K.E.O. and D.G.d.R. were coauthors on a 2016 paper; they worked on different aspects of the study and had no direct collaboration.



[1]To whom correspondence may be addressed. Email: endo-t@biken.osaka-u.ac.jp or dcpage@wi.mit.edu.

[2]Present address: Immunology Frontier Research Center, Research Institute for Microbial Diseases, Osaka University, Suita 565-0871, Japan.

[3]Present address: Metabolon, Inc., Research Triangle Park, NC 27709.

This article contains supporting information online at www.pnas.org/lookup/suppl/doi:10.1073/pnas.1710837114/-/DCSupplemental.

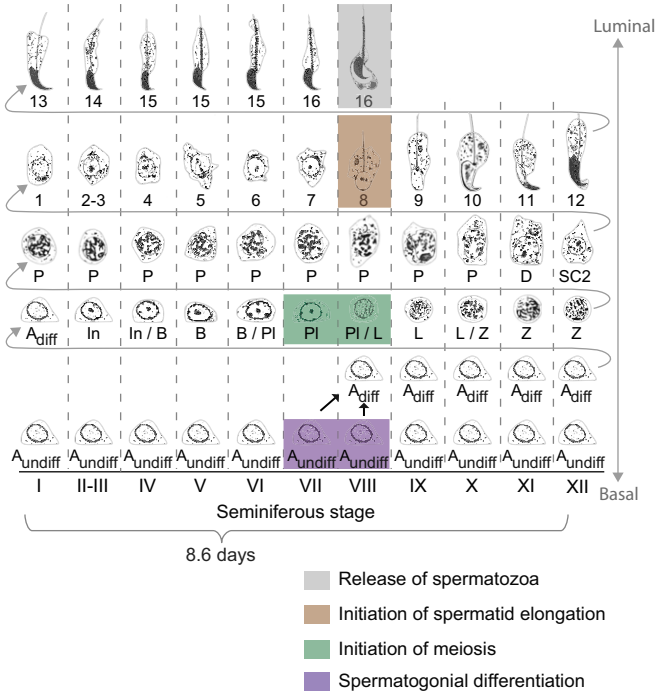


**Fig. 1.** Diagram of mouse spermatogenesis. Oakberg (10) identified 12 distinct cellular associations, called seminiferous stages I to XII. It takes 8.6 d for a section of seminiferous tubule, and the germ cells contained within, to cycle through all 12 stages (9). Four turns of this seminiferous cycle are required for a germ cell to progress from undifferentiated spermatogonium to spermatozoon ready to be released into tubule lumen. $A_{diff}$, differentiating type A spermatogonia; $A_{undiff}$, undifferentiated type A spermatogonia; B, type B spermatogonia; D, diplotene spermatocytes; In, intermediate spermatogonia; L, leptotene spermatocytes; P, pachytene spermatocytes; Pl, preleptotene spermatocytes; SC2, secondary spermatocytes; Z, zygotene spermatocytes. Steps 1 to 16, steps in spermatid differentiation. Purple, germ cells undergoing spermatogonial differentiation; green, meiotic initiation; brown, initiation of spermatid elongation; gray, release of spermatozoa. Adapted from refs. 22 and 62.

of vitamin A. In vitamin A-deficient (VAD) mice and rats, most germ cells arrest as undifferentiated spermatogonia (17, 18). In VAD rat testes, some germ cells also arrest just before meiosis, as preleptotene spermatocytes (19). When VAD animals are given RA or vitamin A, the arrested spermatogonia differentiate (17–19), and the arrested preleptotene spermatocytes initiate meiosis (19). Moreover, deficiency of the RA target gene *Stimulated by retinoic acid gene 8* (*Stra8*), which is expressed exclusively in germ cells (20, 21), causes the failure of meiotic initiation and accumulation of undifferentiated spermatogonia (7, 8, 22). Using *Stra8* as an RA-responsive marker to predict RA levels, we previously reported that rising RA levels coordinate the two premeiotic transitions (22).

Given that the two postmeiotic transitions—initiation of spermatid elongation and release of spermatozoa—coincide with high RA levels, we considered the possibility that RA might also regulate these two transitions. Indeed, ablations of RA receptors (RARs) or RA-synthesizing enzymes (in germ cells and/or Sertoli cells) cause a variety of modest defects in meiotic and postmeiotic aspects of spermatogenesis, including release of spermatozoa (23–29). Nonetheless, the specific steps in meiotic progression or postmeiotic differentiation that RA might regulate have not been established. Moreover, the identity of the cells that supply the RA responsible for premeiotic and/or postmeiotic transitions remains unclear. To explore these questions empirically, we reasoned that we would also need to measure the absolute concentration of RA in testes under a range of experimental conditions.

We first chemically manipulated RA levels in living testes and examined the effects on the two postmeiotic transitions. We then investigated the timing and magnitude of changes in testicular RA concentration by absolute quantification, and we explored which cells provide the RA responsible for these four transitions by genetic and chemical cell depletion assays. We conclude that the two postmeiotic transitions are coordinated by RA produced by pachytene spermatocytes while the two premeiotic transitions are coordinated by RA produced by Sertoli cells.

## Results

**RA Induces Release of Spermatozoa.** We chemically manipulated RA levels in living testes to probe whether RA induces the release of spermatozoa. To ensure the efficacy of our experimental protocols, we first confirmed that i.p. injection of exogenous RA raises the concentration of RA in testes, and, conversely, that injection of WIN18,446, an inhibitor of RA synthesis (30), lowers RA levels in testes. We monitored RA levels in testes both indirectly, by immunostaining for STRA8 as an RA-responsive marker (20, 31, 32), and directly, by measuring RA levels via liquid chromatography/mass spectrometry (LC/MS). In control testis sections, STRA8 protein was not detectable in germ cells in seminiferous stages V and VI (before key transitions) but was clearly present in spermatogonia and preleptotene spermatocytes in stages VII and VIII (during key transitions) (22) (Fig. S2*A*). As expected, at 1 d after a single RA injection, STRA8 was strongly induced in stages V and VI. Conversely, after 2 d of daily WIN18,446 injections, STRA8 was not expressed in stages VII and VIII. LC/MS assays confirmed that RA concentrations in testes were markedly increased 1 d after RA injection and markedly decreased after 2 or 4 d of daily WIN18,446 injection (Fig. 2*A*).

In the unperturbed testis, spermatozoa are released in late stage VIII (Fig. 1). If RA induces this release, then WIN18,446 injection should increase the percentage of seminiferous tubules that contain aligned spermatozoa, which are located along the luminal edge of the seminiferous tubules and are awaiting release into the lumen (Fig. S1*D*). Indeed, this is what we observed: After 2 or 4 d of daily WIN18,446 injection, the percentage of tubule cross-sections containing aligned spermatozoa was increased (Fig. 2 *B–D*, Fig. S2 *B–E*, and *SI Results*); release of spermatozoa was inhibited not only in late stage VIII but also in stages IX and X (Fig. 2*E* and Fig. S2*F*). If this inhibition of spermatozoa release is a consequence of RA depletion, then injection of RA might be expected to induce premature release of spermatozoa. Indeed, at 2 d after a single RA injection, the percentage of tubules containing aligned spermatozoa was decreased, particularly in stage VIII (Fig. 2 *B–D* and Fig. S2 *B–E*). We conclude that RA induces the release of spermatozoa.

**RA Promotes Initiation of Spermatid Elongation.** We then tested whether RA also affects spermatid elongation, the other key postmeiotic transition (Fig. 1). In the unperturbed testis, spermatid development has been subdivided into 16 steps; step 8 round spermatids initiate their elongation in stage VIII and become step 9 elongating spermatids in stage IX (Fig. 1). If RA induces this initiation of spermatid elongation, then WIN18,446 injection should increase the percentage of seminiferous tubules that contain step 7 and 8 round spermatids. Indeed, following 2 or 4 d of daily WIN18,446 injection, the percentage of tubules containing step 7 and 8 round spermatids was increased, and the percentage of tubules containing step 9 and 10 elongating spermatids was correspondingly decreased (Fig. 3 *A* and *B*). Extending these daily injections to 21 d resulted in a nearly complete arrest at step 7 and 8 round spermatids (Fig. S3*A* and *SI Results*). By contrast, at 2 d after a single RA injection, the percentage of tubules containing step 7 and 8 round spermatids was decreased, and the percentage of tubules containing step 9 and 10 elongating spermatids was correspondingly increased (Fig. 3 *A* and *B*). These quantitative results indicate that initiation of spermatid elongation is regulated by RA.

We next used pulse–chase labeling (33, 34) to confirm that RA causes spermatid elongation to be initiated earlier than it would normally occur. When a single BrdU injection is given, BrdU is incorporated into cells in mitotic or premeiotic S phase. At 4 h after BrdU injection, the most advanced BrdU-labeled germ cells are

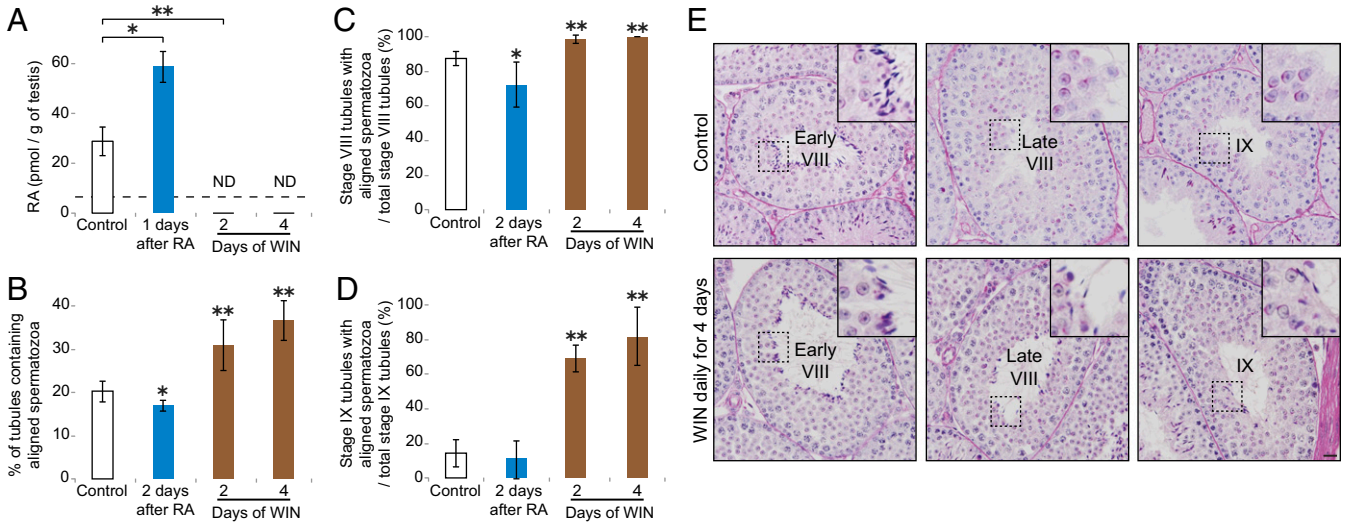


**Fig. 2.** RA induces release of spermatozoa. (*A*) Absolute quantification of RA concentrations (pmol/g of testes) in control and RA-injected and WIN18,446-injected adult testes. Mice were given a single dose of RA or daily injections of WIN18,446 for 2 or 4 d. Dashed line, limit of detection. ND, not detected (below limit of detection). Bar graphs after RA or WIN18,446 treatment show results of two biological replicates. Error bars, mean ± SD, $*P < 0.05$, $**P < 0.01$, compared with control (one-tailed *t* test). (*B*) Percentage of testis tubule cross-sections containing aligned spermatozoa, in controls, or 2 d after single RA injection, or after 2 or 4 d of daily WIN18,446 (WIN) injection. Error bars, mean ± SD, $*P < 0.05$, $**P < 0.01$, compared with control (one-tailed *t* test). (*C* and *D*) Number of stage VIII (*C*) or stage IX (*D*) tubule cross-sections with aligned spermatozoa per total stage VIII (*C*) or stage IX (*D*) tubule cross-sections, in controls, or 2 d after single RA injection, or after 2 or 4 d of daily WIN18,446 injection. Error bars, mean ± SD, $*P < 0.05$, $**P < 0.01$, compared with control (one-tailed *t* test). (*E*) Control (*Top*) and WIN18,446-injected (*Bottom*) testis cross-sections in early stage VIII (*Left*), late stage VIII (*Middle*), and stage IX (*Right*), stained with hematoxylin and periodic acid-Schiff (He-PAS). *Insets* (65.5 μm × 65.5 μm) enlarge boxed regions. (Scale bar: 30 μm.)

preleptotene spermatocytes that have undertaken premeiotic S and thereby initiated the meiotic program (Fig. S3 *B* and *C*). In the unperturbed testis, these BrdU-labeled preleptotene spermatocytes develop into step 8 round and step 9 and 10 elongating spermatids, respectively, 17.2 and 18.2 d after BrdU injection (Fig. 3*C*). We predicted that RA or WIN18,446 treatment would accelerate or delay spermatid development, respectively, at 18.2 d after the BrdU labeling, when the most advanced BrdU-labeled germ cells in unperturbed testes have initiated spermatid elongation. To test this, we gave mice a single BrdU injection, followed by daily RA or WIN18,446 injection during spermatid development (Fig. 3*C*), and harvested the testes at 17.2 d (Exps. 1 to 3) or 18.2 d (Exps. 4 to 6). We found that, at 17.2 d after BrdU injection, the most advanced BrdU-labeled germ cells were step 8 round spermatids in control testes, and there was no acceleration or delay under RA or WIN18,446 treatment (Fig. S3 *D* and *F*). This demonstrates that RA does not affect the development of round spermatids, from step 1 to step 8. However, as predicted, at 18.2 d after BrdU injection, the most advanced BrdU-labeled germ cells, which were step 10 spermatids in controls, had developed further—into step 11 spermatids—in RA-treated testes whereas they were still step 9 spermatids in WIN18,446-treated testes (Fig. 3*D* and Fig. S3*F*). Taken together, these findings provide strong evidence that RA promotes the initiation of spermatid elongation.

**RA Has No Discernible Effect on Meiotic Progression.** Given that four of the five generations of spermatogenic cells undergo transitions coregulated by RA in stages VII and VIII (Fig. 1), we wondered whether the remaining cell type at these stages, pachytene spermatocytes, also undergoes RA-regulated development during meiotic progression.

We examined this possibility by pulse–chase labeling. We gave mice a single injection of BrdU, followed by daily RA or WIN18,446 injection during meiotic progression (Fig. 3*C*, Exps. 7 to 9), and harvested the testes at 12.6 d, when, in control testes, the most advanced BrdU-labeled germ cells have completed meiotic progression and become step 1 and 2 spermatids. At 12.6 d, there was no acceleration or delay under RA or WIN18,446 treatment (Fig. S3 *E* and *F*). These results indicate that RA does not affect meiotic progression as assayed histologically.

To verify that RA does not affect meiotic progression at the molecular level, we tested for key molecular features of meiotic progression by immunohistochemistry. We first gave mice a single injection of 5-ethynyl-2′-deoxyuridine (EdU), followed by daily RA or WIN18,446 injection during meiotic progression (Fig. 4*A*), and harvested testes at 8.6 d (Exps. 10 to 12) and 11 d (Exps. 13 to 15), when in control testes the most advanced EdU-labeled germ cells have progressed to late pachytene stage and diplotene stage, respectively (35). We then immunostained the EdU-labeled nuclear spreads of spermatocytes for markers of meiotic prophase to distinguish among middle pachytene, late pachytene, and diplotene stages. Specifically, we used antibodies against phosphorylated H2A histone family member X (γH2AX) (a marker of DNA double strand breaks and sex body formation) (36), synaptonemal complex protein 3 (SYCP3) (a marker of synaptonemal complex) (37), testis-specific histone (H1t) (a marker of middle/late pachytene stages) (38), and ataxia telangiectasia and Rad3-related protein (ATR) (a marker of DNA repair and sex body formation) (39). Based on these markers (*SI Results*), at 8.6 d and 11 d after EdU injection, the most advanced EdU-labeled germ cells in control testes were, respectively, late pachytene and diplotene spermatocytes, and there was no acceleration or delay after RA or WIN18,446 treatment (Fig. 4 *B–D* and Fig. S4). Importantly, expression and localization of all of the meiotic markers appeared to be unaffected by either RA or WIN18,446 treatment. We conclude that RA has no discernible effect on meiotic progression from leptotene stage to diplotene stage, including the development of pachytene spermatocytes.

Our results demonstrate that RA regulates release of spermatozoa and initiation of spermatid elongation, as well as spermatogonial differentiation and meiotic initiation, but not meiotic progression, in stages VII and VIII. To explore the mechanism by which these four transitions are coordinated in time and space by RA, we next focused on changes in RA levels in the seminiferous tubules.

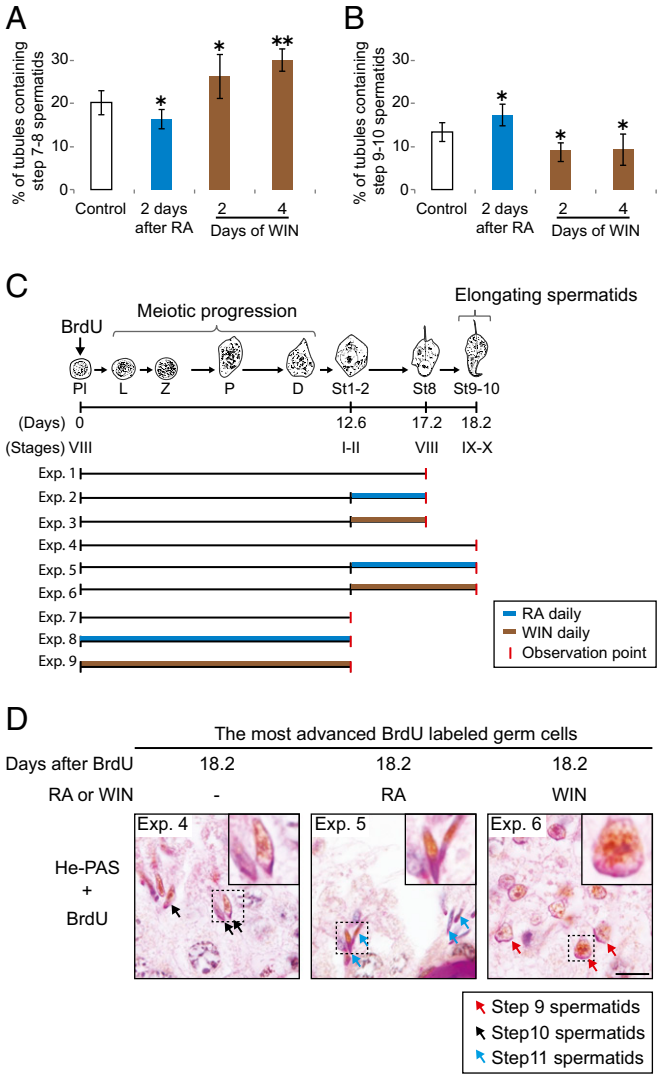


**Fig. 3.** RA promotes initiation of spermatid elongation. (*A* and *B*) Percentage of testis tubule cross-sections containing step 7 and 8 (*A*) or step 9 and 10 (*B*) spermatids, in controls, or 2 d after single RA injection, or after 2 or 4 d of daily WIN18,446 injection. Error bars, mean ± SD, $*P < 0.05$, $**P < 0.01$, compared with control (one-tailed *t* test). (*C*) Diagram of predicted development of most advanced BrdU-labeled germ cells following single BrdU injection. Mice received daily injections of RA or WIN18,446 until the observation points, when testes were harvested (Exps. 1 to 9). D, diplotene spermatocytes; L, leptotene spermatocytes; P, pachytene spermatocytes; Pl, preleptotene spermatocytes; Z, zygotene spermatocytes. St1-2, St8, and St9–10: steps in spermatid differentiation. (*D*) The most advanced BrdU-labeled germ cells in testis cross-sections of control (*Left*), RA-injected (*Middle*), or WIN18,446-injected (*Right*) mice 18.2 d (Exps. 4 to 6) after single BrdU injection, immunostained for BrdU with hematoxylin and periodic acid-Schiff (He-PAS) staining. *Insets* (7.5 μm × 7.5 μm) enlarge boxed regions. Arrows: step 9 (red), step 10 (black), step 11 (blue) spermatids. (Scale bar: 10 μm.)

**RA Concentrations Change Periodically, as Reflected by STRA8 Expression Patterns.** We previously reported that STRA8, an RA responsive marker, is expressed periodically in the unperturbed testis: Expression of the protein is low or absent in spermatogonia in stages II to VI, increased in stages VII and VIII, and remains high in stages IX to I (22). Thus, we postulated that the STRA8 expression patterns reflect periodic changes in RA levels: RA levels might rise in stages VII and VIII, to coordinate the four transitions, and remain high until stages XII/I. To test these predictions, we quantified RA concentrations in seminiferous stage-synchronized testes by LC/MS.

In unperturbed mouse testes, the seminiferous stages of the tubules are not synchronized across the testis but instead are highly diverse (40) (Fig. S1*B*). When mice are treated daily with WIN18,446 from postnatal day 2 (P2), germ cells arrest as undifferentiated spermatogonia at stages VII and VIII (41) (Fig. 1). After a single injection of RA into these WIN18,446-pretreated mice, the arrested germ cells undergo spermatogonial differentiation to initiate spermatogenesis in a synchronized manner (41). Thus, we gave daily injections of WIN18,446 from P2 until P14 (Fig. S5*A* and *SI Results*) and then injected a single dose of RA at P15, harvesting testes 5, 8, 9, or 10 d after the RA injection (Fig. 5*A* and Fig. S5*B*). As we anticipated, at 5 d after RA injection, when seminiferous tubules were synchronized at stages II to IV, the RA concentration was negligible or very low (Fig. 5*B* and Fig. S5*D*). Then, at 8 d, in stages VII to IX, the RA concentration was significantly increased, and it remained high at 9 d, in stages IX to XI, before falling modestly at 10 d, in stages XI to I (difference between RA levels in stages VII to IX and XI to I is not significant; $P > 0.05$, Tukey–Kramer test). We conclude that RA concentrations change periodically, as also reflected by, and in good agreement with, STRA8 expression patterns (Fig. S5*C*).

**RA Concentration Increases When *Aldh1a2*-Expressing Pachytene Spermatocytes First Appear.** We then considered the identity of the cells within the seminiferous tubules that produce RA. Sertoli cells, which have been shown to express an RA-synthesizing enzyme, aldehyde dehydrogenase 1A1 (*Aldh1a1*) (42, 43), are likely the source of the RA measured in the experiments just described. Another RA-synthesizing enzyme, *Aldh1a2*, is abundantly expressed in pachytene spermatocytes (and their descendants, diplotene spermatocytes) from stages VII through XII (42, 43). If pachytene spermatocytes actually produce RA from stage VII onward, then RA levels in the testes of young males should rise shortly after these *Aldh1a2*-expressing pachytene cells first appear (at about 15 d after RA-induced spermatogonial differentiation). To test this prediction, we harvested stage-synchronized testes at 12, 15, 16, and 17 d after RA injection, when pachytene and then diplotene spermatocytes first appear (Fig. 5*A* and Fig. S5*B*), for absolute quantification of RA levels. At 12 d after RA injection, when seminiferous tubules containing pachytene spermatocytes were in stages II to IV, RA concentration was very low, similar to 5 d after RA injection (Fig. 5*B* and Fig. S5*D*). As predicted, at 15 d after RA injection, in stages VII to IX, RA concentration was increased and significantly higher than at 8 d, when pachytene spermatocytes were not yet present. The higher RA concentration was maintained at 16 d and 17 d, in stages IX to XI and stages XI to I, respectively. The simplest interpretation of these data is that pachytene spermatocytes not only express *Aldh1a2* but also produce RA from stages VII and VIII onward.

**Depletion of Pachytene Spermatocytes Reduces RA Concentration in Adult Testes.** Building upon these findings, we hypothesized that RA produced by pachytene spermatocytes might induce or contribute to some of the key germ cell transitions that occur in stage VII and VIII tubules (Fig. 1). To explore the functional roles of RA produced by pachytene spermatocytes, we conditionally removed pachytene spermatocytes from adult testes, using a cell depletion assay. Hydroxyurea (HU) specifically inhibits the ribonucleotide reductase that generates deoxyribonucleotides required for DNA replication, by binding the enzyme's iron molecules, thereby killing cells that are in S phase (44, 45). We injected adult mice with HU six times, at 6-h intervals, and we first assessed the results of HU treatment at 36 h (1.5 d) after the initial injection. As expected, all differentiating spermatogonia ($A_1/A_2/A_3/A_4$/intermediate/B spermatogonia) and stage VII preleptotene spermatocytes had been eliminated by HU treatment (Fig. 5*C*, Fig. S6*A*, and *SI Results*), with no cytotoxic effects on the remaining germ cells, or on Sertoli cells (46). At 11.6 d after the first HU injection, the specific cohort of germ cells that normally would have transited to pachytene and diplotene in stages I to XII was missing from the testis, as expected (Fig. 5*C* and Fig. S6*B*); in stage VII and VIII tubules, pachytene spermatocytes were the

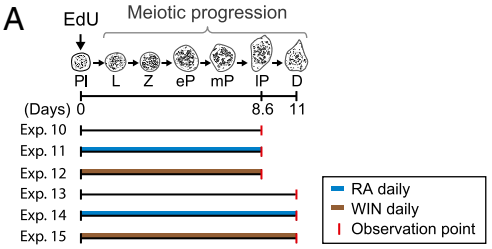


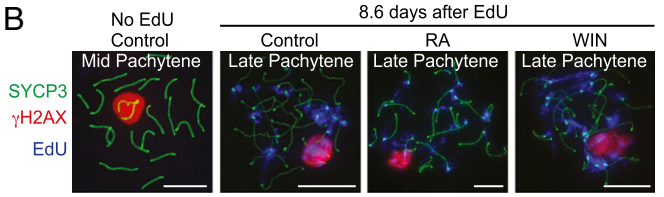


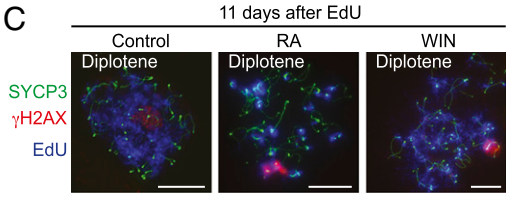


D

| Days after EdU | Treatment | Middle pachytene | | Late pachytene | | Diplotene | | Total cells counted |
|---|---|---|---|---|---|---|---|---|
| | | Cells counted | EdU+ cells (%) | Cells counted | EdU+ cells (%) | Cells counted | EdU+ cells (%) | |
| 8.6 | Cont | 68 | 23 (33.8) | 91 | 47 (51.6) | 35 | 0 (0) | 194 |
| 8.6 | RA | 108 | 41 (38.0) | 113 | 59 (52.2) | 29 | 0 (0) | 250 |
| 8.6 | WIN | 139 | 51 (36.7) | 132 | 70 (53.0) | 31 | 0 (0) | 302 |
| 11.0 | Cont | 89 | 27 (30.3) | 115 | 46 (40.0) | 83 | 63 (75.9) | 287 |
| 11.0 | RA | 90 | 30 (33.3) | 91 | 36 (39.6) | 80 | 57 (71.3) | 261 |
| 11.0 | WIN | 34 | 11 (32.4) | 89 | 35 (39.3) | 84 | 62 (73.8) | 208 |

**Fig. 4.** RA has no discernible effect on meiotic progression after entry into meiotic prophase. (*A*) Diagram of predicted development of most advanced EdU-labeled germ cells following single EdU injection. Mice received daily injections of RA or WIN18,446 until the observation point, when testes were harvested (Exps. 10 to 15). D, diplotene spermatocytes; eP, early pachytene spermatocytes; L, leptotene spermatocytes; lP, late pachytene spermatocytes; mP, mid pachytene spermatocytes; Pl, preleptotene spermatocytes; Z, zygotene spermatocytes. (*B* and *C*) The most advanced EdU-labeled germ cells in nuclear spreads of spermatocytes in control or daily RA- or WIN18,446-injected mice at 8.6 d (*B*; Exps. 10 to 12; late pachytene stage) or 11 d (*C*; Exps. 13 to 15; diplotene stage) after a single EdU injection, immunostained for SYCP3 (green), γH2AX (red), and EdU (blue). (*B*, *Far Left* ) Representative mid-pachytene spermatocyte showing no EdU signal in controls. (Scale bars: 10 μm.) (*D*) Numbers and percentages of mid-pachytene, late pachytene, and diplotene cells positive for EdU. Percentages of $EdU^+$ cells did not differ significantly among control, RA-treated, and WIN-treated groups (three biological replicates; $P > 0.05$; $\chi^2$ test).

only missing cells, again as expected (Fig. 5*D* and Fig. S6*C*). Importantly, testicular RA concentrations were significantly lower than in controls (Fig. 5*E* and Fig. S6 *D* and *E*). Also, as predicted, we observed that the remaining levels of RA, which probably derived from Sertoli cells, were eliminated by coinjection of WIN18,446 with HU. We conclude that conditional depletion of pachytene spermatocytes reduces RA levels in adult testes.

To confirm that the reduced RA concentration at 11.6 d after the first HU injection was associated with the depletion of a specific RA-synthesizing enzyme from seminiferous tubules, we carried out single-molecule fluorescence in situ hybridization (smFISH). Because smFISH probes detect and localize each target mRNA molecule as a punctate signal, these signals can be quantified to determine the number of transcripts per cell (47) (*SI Results*). In control stage VII and VIII tubules, *Aldh1a2* was expressed specifically in pachytene spermatocytes, *Aldh1a1* was expressed specifically in Sertoli cells, and *Aldh1a3* was expressed at very low levels, if at all, in germ cells and Sertoli cells (Fig. 6), all as previously reported (42, 43); we used kidney as a positive control for *Aldh1a3* (Fig. S7 *E* and *F* and *SI Results*). As predicted, at 11.6 d after the first HU injection, *Aldh1a2* transcripts were dramatically reduced in seminiferous tubules, likely because of the absence of pachytene spermatocytes. Importantly, we observed no compensatory up-regulation of *Aldh1a1*, *Aldh1a2*, or *Aldh1a3* in the remaining germ or Sertoli cells of the seminiferous tubules, despite the fact that such compensation has been observed to accompany genetic ablation of these genes in other contexts (48, 49). Conversely, HU depletion of pachytene spermatocytes did not result in reduced expression of *Aldh1a1*, *Aldh1a2*, or *Aldh1a3* in the remaining germ or Sertoli cells. Thus, the reduction in RA concentration upon depletion of pachytene spermatocytes was not due to reduced expression of RA-synthesizing enzymes in the remaining cells of the seminiferous tubules. Instead, depletion of ALDH1A2-expressing pachytene spermatocytes reduces testicular RA concentrations directly. We then proceeded to test whether RA from pachytene spermatocytes contributes functionally to the four key transitions in stages VII and VIII, using HU-treated testes.

**RA from Pachytene Spermatocytes Is Required for Postmeiotic, but Not for Premeiotic, Transitions.** If RA from pachytene spermatocytes is required for release of spermatozoa and initiation of spermatid elongation, seminiferous tubules should display accumulations of aligned (unreleased) spermatozoa and round (unelongated) spermatids, respectively, at 11.6 d after the first HU injection. Indeed, at 11.6 d after the first HU injection, seminiferous tubules displayed increased numbers of aligned spermatozoa and step 7 and 8 round spermatids (Fig. 7 *A* and *B* and Fig. S8 *A–D*). These accumulations of unreleased spermatozoa and unelongated spermatids in response to HU were not exacerbated by coinjecting WIN18,446 with HU. Moreover, when a single dose of RA was injected 9.6 d after the first HU injection, the abnormal accumulations were cured, or rescued, at 11.6 d, indicating that the accumulations after pachytene spermatocyte depletion were due specifically to the resulting decrease in RA concentration. We conclude that RA from pachytene spermatocytes is required for initiation of spermatid elongation and for release of spermatozoa.

We next tested whether RA from pachytene spermatocytes is required for meiotic initiation. At 11.6 d after the first HU injection, both preleptotene spermatocytes and type A spermatogonia in stages VII and VIII expressed *Stra8* (transcripts) at levels similar to those of

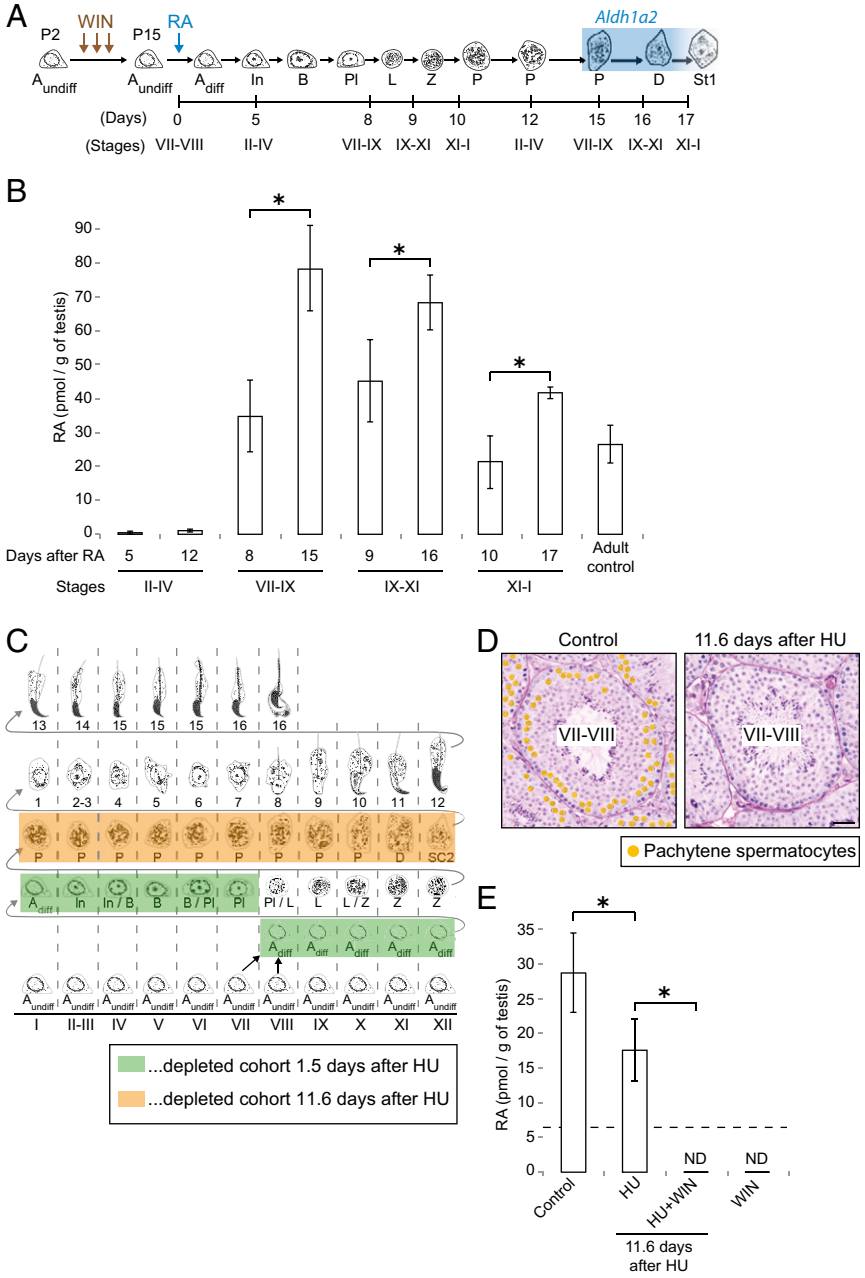


**Fig. 5.** RA concentrations change periodically, and RA derives in part from pachytene spermatocytes. (*A*) Diagram of synchronous germ cell development after RA-induced spermatogonial differentiation in WIN18,446-pretreated young mice. Mice were given daily injections of WIN18,446 from postnatal day 2 (P2) until P14 and were then given a single dose of RA at P15. Testes were harvested at the indicated days after the RA injection. Blue, high *Aldh1a2* expression (43). $A_{diff}$, differentiating type A spermatogonia; $A_{undiff}$, undifferentiated type A spermatogonia; B, type B spermatogonia; D, diplotene spermatocytes; In, intermediate spermatogonia; L, leptotene spermatocytes; P, pachytene spermatocytes; Pl, preleptotene spermatocytes; Z, zygotene spermatocytes. St1, step 1 spermatids. (*B*) Absolute quantification of RA levels (pmol/g of testes) in synchronized (WIN18,446/RA-injected) young testes. Bar graphs at 12, 15, 16, and 17 d after RA injection show results of two biological replicates. Error bars, mean ± SD, $*P < 0.05$ (one-tailed *t* test). (*C*) Germ cell depletion after hydroxyurea (HU) injection. Mice received six injections of HU at 6-h intervals. Boxes, completely depleted germ cell cohort 1.5 d (green) or 11.6 d (orange) after first HU injection. (*D*) Testis cross-sections in stages VII and VIII of control (*Left*) or HU-injected (*Right*) mice, stained with hematoxylin and periodic acid-Schiff (He-PAS). Orange dots, pachytene spermatocytes. (Scale bar: 30 μm.) (*E*) Quantification of RA levels (pmol/g of testes) in testes of control and HU-injected adult mice. HU + WIN, mice were given injections of HU and then daily injections of WIN18,446, beginning 7.6 d after first HU injection. WIN, mice received daily injections of WIN18,446 for 4 d. Dashed line, limit of detection. ND, not detected (below limit of detection). The far right "WIN" bar graph shows results of two biological replicates. Error bars, mean ± SD, $*P < 0.01$ (Tukey–Kramer test).

controls (Fig. 6*A* and Fig. S7*D*), suggesting that these germ cells are responding normally, to endogenous RA, even in the absence of pachytene spermatocytes and the RA that they provide. If RA from pachytene cells is not required for meiotic initiation, then premeiotic or early meiotic (leptotene) spermatocytes should not be increased or decreased after pachytene spermatocyte depletion. Indeed, at 11.6 d after the first HU injection, there was no increase in the numbers of tubules containing premeiotic (preleptotene) spermatocytes or decrease in the numbers of tubules containing early meiotic (leptotene) spermatocytes (Fig. 7*C* and Fig. S8 *A*, *B*, *E*, and *F*). Similarly, we confirmed that genetic depletion of pachytene spermatocytes, in *Dmc1*- or *Spo11*-deficient mice, had no discernible effect on preleptotene or leptotene spermatocytes; in these mutant mice, defects in meiotic progression result in apoptosis of pachytene spermatocytes before or during stage IV (50–53). By contrast, coinjection of WIN18,446 with HU did increase preleptotene spermatocytes and decrease leptotene spermatocytes, and coinjection of RA with HU decreased preleptotene spermatocytes and increased leptotene spermatocytes. These results suggest that meiotic initiation requires RA from sources other than pachytene spermatocytes.

Finally, we tested whether RA from pachytene spermatocytes is required for spermatogonial differentiation, by immunostaining for functional markers of spermatogonial differentiation, STRA8 and KIT (22, 54). As mentioned above, at 11.6 d after the first HU injection, type A spermatogonia in stages VII and VIII expressed *Stra8* (transcripts) at levels like those seen in controls (Fig. 6*A* and Fig. S7*D*). Similarly, we found that expression of the STRA8 and KIT proteins in spermatogonia was unaffected in stages VII and VIII at 11.6 d after the first HU injection (Fig. 7*D*). By contrast, STRA8 and KIT were not expressed in these cells following coinjection of WIN18,446 with HU, suggesting that spermatogonial differentiation also requires RA from sources other than pachytene spermatocytes. We conclude that RA from pachytene spermatocytes is required for initiation of spermatid elongation and release of spermatozoa, but not for spermatogonial differentiation or meiotic initiation (Fig. 8).

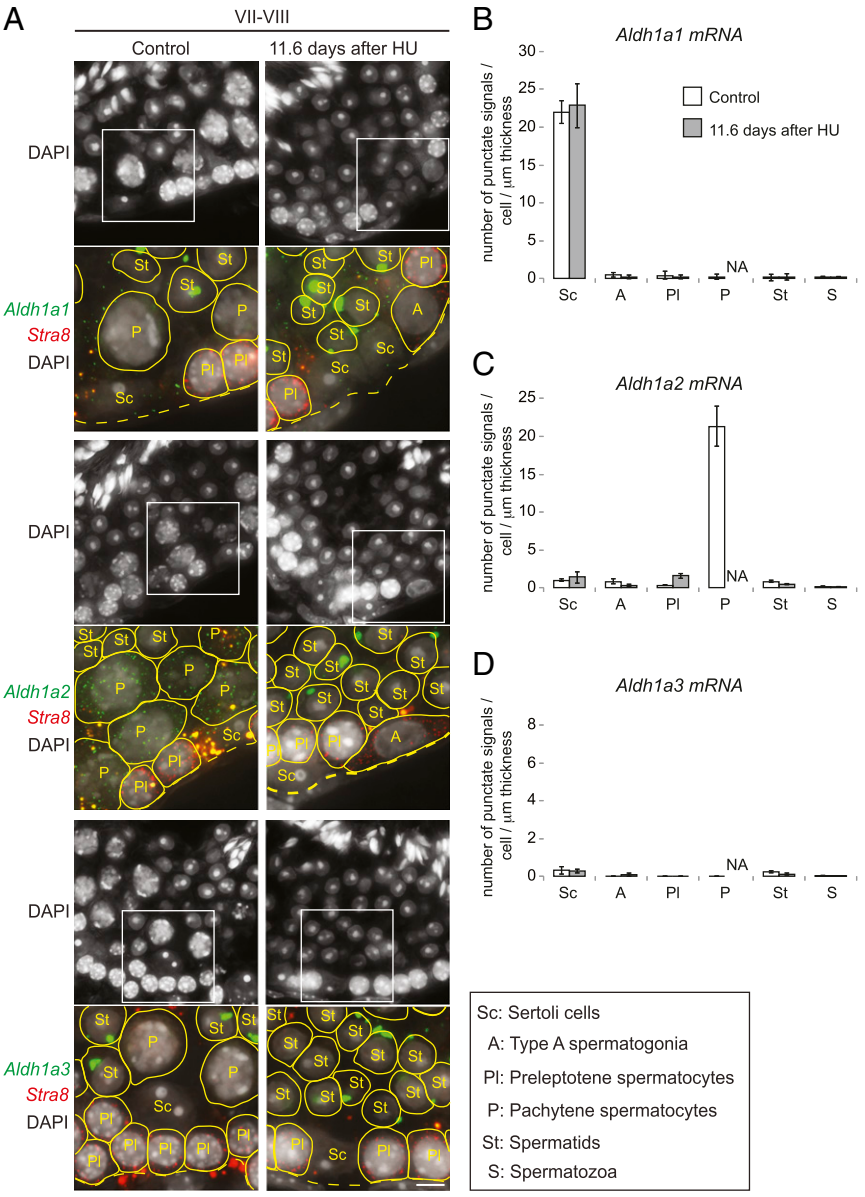


**Fig. 6.** Depletion of pachytene spermatocytes reduces *Aldh1a2* expression in seminiferous tubules. (*A*) Single-molecule fluorescence in situ hybridization (smFISH) for mRNAs of *Aldh1a1* (green), *Aldh1a2* (green), *Aldh1a3* (green), and *Stra8* (red), with DAPI counterstain (gray), on testis cross-sections in stages VII and VIII of control and HU-injected mice. Single transcripts are visible as punctate signals. Large spots in round spermatids are nonspecific signals (*SI Results*). Yellow spots in merged images are autofluorescent signals. Boxed regions (32.5 μm × 32.5 μm) in DAPI images (65 μm × 65 μm) indicate areas shown in higher magnification below each image. Yellow lines encircle germ cells, according to the cell borders visualized by overexposed images (see Fig. S7 *A* and *B* for details). A, type A spermatogonia; dashed lines, basal laminae of tubule cross-sections; Pl and P, preleptotene and pachytene spermatocytes; Sc, Sertoli cells; St, spermatids. (Scale bar: 5 μm.) (*B–D*) Number of smFISH punctate signals per cell per 1-μm section thickness for *Aldh1a1* (*B*), *Aldh1a2* (*C*), and *Aldh1a3* (*D*) mRNA, in controls or 11.6 d after first HU injection. Error bars, mean ± SE. A, type A spermatogonia; NA, not applicable because no pachytene spermatocytes were present; Pl and P, preleptotene and pachytene spermatocytes; S, spermatozoa; Sc, Sertoli cells; St, spermatids.

## Discussion

**RA Regulates Four Key Transitions of Spermatogenesis.** We investigated the chemical basis of the exquisite coordination of spermatogenesis, the process by which diploid spermatogonia differentiate into specialized haploid gametes, spermatozoa, at a constant rate. We found that rising levels of an extrinsic signal, RA, regulate four key developmental transitions in mouse spermatogenesis: spermatogonial differentiation and meiotic initiation before meiosis (22) and initiation of spermatid elongation and release of spermatozoa after meiosis (Fig. 8*A*). We also found that these pre- and postmeiotic transitions require RA from different cell sources: Sertoli (somatic) cells and pachytene spermatocytes (meiotic cells), respectively (Fig. 8*B*). We will now discuss the implications of these findings for understanding the regulation of this temporally and spatially coordinated system of cell division and differentiation (10, 14).

By chemically manipulating the levels of RA in the testes of live animals, we found that RA plays critical, primary roles in the two postmeiotic transitions: initiation of spermatid elongation and release of spermatozoa. Indeed, both of these transitions were inhibited within 2 d after starting injections of a potent inhibitor of RA synthesis, WIN18,446. Conversely, injection of RA was sufficient to induce both of these postmeiotic transitions, again within 2 d. These findings align with, and help explain, prior reports of postmeiotic defects caused by genetic or chemical ablation of RA receptors (RARs) or RA-synthesizing enzymes (23–29). Further, we found that, after meiotic initiation, progression and completion of meiosis and subsequent development of round spermatids are unaffected by manipulations of RA levels, suggesting that RA plays little or no direct role in this middle, 17-d stretch of spermatogenesis. Because RA also coregulates the two premeiotic transitions (17–19, 22), our present findings demonstrate that four of the five generations of spermatogenic cells present in stage VII and VIII tubules undergo transitions regulated by a single extrinsic cue, RA.

It remains to be determined whether RA acts directly on germ cells or indirectly, via Sertoli cells, to regulate the two postmeiotic transitions. RA serves as a ligand to nuclear receptors known as RARs and retinoid X receptors (RXRs), which bind to RA response elements (RAREs) in the regulatory regions of target genes (55). These receptors are expressed specifically in round spermatids in stages VII and VIII (during key transitions) (42), suggesting that RA acts directly on round spermatids to induce their elongation. Indirect RA signaling, via RARs/RXRs in Sertoli cells (42), may also contribute to

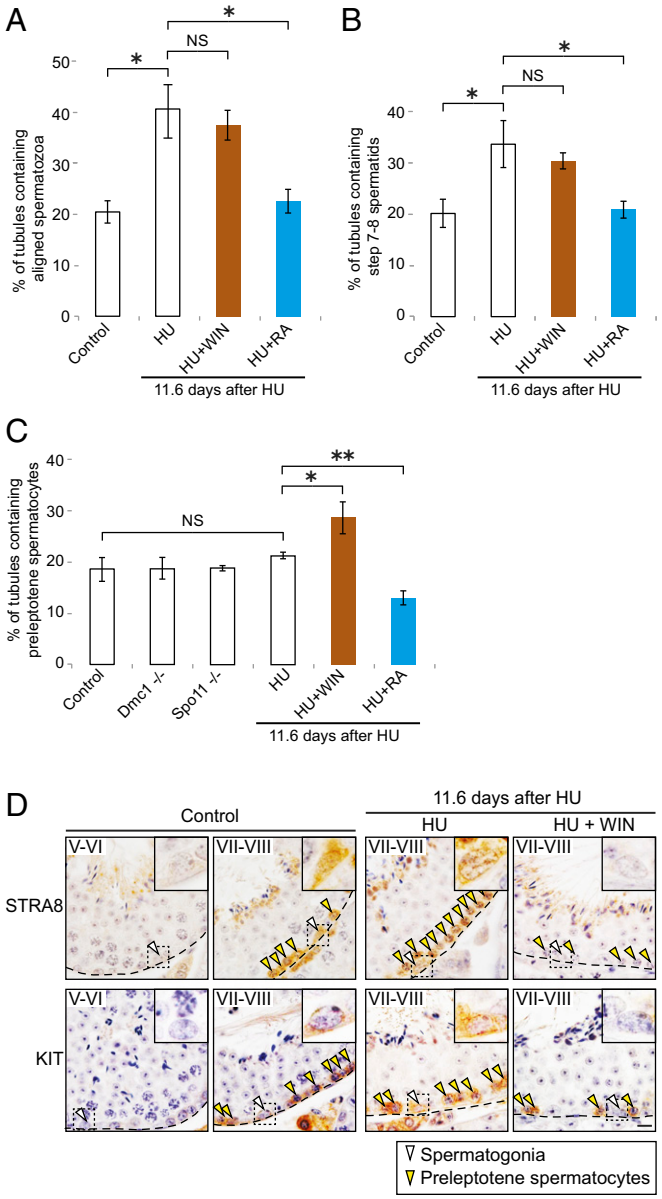


**Fig. 7.** RA from pachytene spermatocytes is required for postmeiotic but not premeiotic transitions. (*A* and *B*) Percentage of testis tubule cross-sections containing aligned spermatozoa (*A*) and step 7 and 8 spermatids (*B*), in controls or 11.6 d after first HU injection. HU + WIN: mice were given injections of HU and then daily injections of WIN18,446, beginning 7.6 d after first HU injection. HU + RA, mice received single dose of RA, 9.6 d after first HU injection. Error bars, mean ± SD, $*P < 0.01$ (Tukey–Kramer test). NS, not significant ($P > 0.05$). (*C*) Percentage of testis tubule cross-sections containing preleptotene spermatocytes, in controls or 11.6 d after first HU injection, and in *Dmc1*- or *Spo11*-deficient testes. Error bars, mean ± SD, $*P < 0.05$, $**P < 0.01$ (Tukey–Kramer test). NS, not significant ($P > 0.05$). (*D*) Immunostaining for STRA8 and KIT on control or HU-injected testis cross-sections. Roman numerals indicate stages. *Insets* (14.5 μm × 14.5 μm) enlarge boxed regions. Dashed lines, basal laminae of tubule cross-sections. Arrowheads, spermatogonia (white) and preleptotene spermatocytes (yellow). (Scale bar: 10 μm.)

this process. By contrast, RA is likely to regulate release of spermatozoa indirectly, via Sertoli cells, because spermatozoa are understood to be transcriptionally silent (56). Given that release of spermatozoa is the process by which spermatozoa and Sertoli cells disengage from each other, spermatozoa may be released passively, through RA function in Sertoli cells. It will be useful to conduct studies to determine whether RA regulates each of these two postmeiotic transitions directly or indirectly, by searching for RA target genes yet to be identified.

**RA Concentrations Change Periodically, as Reflected by STRA8 Expression Patterns.** Recent studies have addressed the question of whether RA levels fluctuate in the testis to regulate the 8.6-d cycle of spermatogenesis. Insights into the question have emerged from studies of *Aldh1a* gene expression, RAR receptor function, and relative measurements of RA levels (27, 43, 57). However, the actual concentrations of RA in testes, and their dynamics and range, remained unclear. We previously reported that the RA-responsive marker STRA8 is expressed periodically in the unperturbed testis, and, on this basis, we postulated that RA levels rise and fall periodically (22). By absolute quantification of RA levels, we now provide direct evidence that RA levels change periodically and that these changes are mirrored by changes in STRA8 expression: RA levels are low in stages II to VI, rise in stages VII and VIII, and remain high until stages XII/I. This long elevation of RA levels in stages VII to XII/I is consistent with other published expression data and functional studies (27, 42, 43). By contrast, Hogarth et al. (57) suggested, based on relative RA measurement, a sharp peak in RA levels in stages VIII and IX. This difference between Hogarth et al.'s findings and those reported here likely reflects differences in experimental designs and in methods of measurement and analysis employed. For example, while we analyzed stage-synchronized testes between 5 and 17 d after RA injection, Hogarth et al. analyzed testes between 42 and 50 d after RA injection, by which point synchrony may be less consistent (41, 58).

Our findings demonstrate that, in the unperturbed testis, RA concentrations rise in stages VII and VIII, thereby coordinating four spermatogenic transitions, and they remain elevated until stages XII/I. We previously showed that germ cells have stage-limited competencies to undergo spermatogonial differentiation and meiotic initiation (22). These windows of competence begin while RA levels are low, and end (in stage VIII) while RA levels are still high, so that the competencies intersect with high RA levels briefly to confine the timing of premeiotic transitions (to stages VII and VIII). It remains to be determined whether round spermatids have a similarly limited competency (ending in stage VIII) to undertake the initiation of spermatid elongation (in stages VII and VIII).

**Periodic RA from Sertoli Cells and Pachytene Spermatocytes Coordinates Four Transitions.** Based on the observation that an RA-synthesizing enzyme, *Aldh1a2*, is expressed in pachytene spermatocytes (42, 43) and that spermatogonial differentiation requires RA, Sugimoto et al. (43) hypothesized that production of RA by pachytene spermatocytes induces the next round of spermatogonial differentiation. Indeed, we found that RA concentrations increase when *Aldh1a2*-expressing pachytene spermatocytes first appear in young males (Fig. 5*B*), consistent with Sugimoto et al.'s suggestion that pachytene spermatocytes produce RA. However, using genetic and chemical cell depletion assays, we showed that RA from pachytene spermatocytes is required for postmeiotic transitions, but not for premeiotic transitions. Based on the findings reported here, we propose that pre- and postmeiotic transitions are regulated by RA from different sources. Specifically, the model posits that Sertoli cells periodically produce RA to regulate two premeiotic transitions and that pachytene spermatocytes produce RA to regulate two postmeiotic transitions. Several observations support the model that these premeiotic transitions are coordinated by RA from Sertoli cells (but not from pachytene spermatocytes). First, Sertoli cell-specific ablations of *Aldh1a1-3* cause an arrest of the first spermatogonial differentiation in postnatal mice (28). Second, using RA quantification, we now show that RA periodicity (with rising RA concentrations in stages VII and VIII) is maintained even in the absence of pachytene spermatocytes. Further, we provide both chemical and genetic evidence that depletion of pachytene spermatocytes does not affect the timing of the premeiotic transitions: These timed transitions are maintained in *Dmc1*- and *Spo11*-deficient males, in which pachytene spermatocytes are

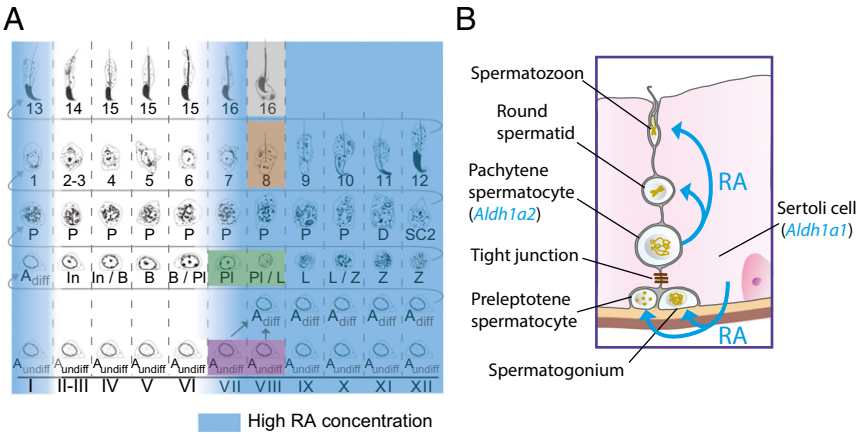


**Fig. 8.** A proposed model by which RA coordinates spermatogenesis. (*A*) Periodic RA signaling coordinates four transitions. Blue, high RA concentration; purple, spermatogonial differentiation; green, meiotic initiation; brown, initiation of spermatid elongation; gray, release of spermatozoa. (*B*) Sertoli cells express *Aldh1a1* to produce RA required for spermatogonial differentiation and meiotic initiation. Pachytene spermatocytes express *Aldh1a2* to produce RA required for initiation of spermatid elongation and release of spermatozoa.

depleted. Finally, Sertoli cells establish a stage-dependent cycle of metabolism in neonatal males, before pachytene spermatocytes first appear (59), leading us to propose that Sertoli cells may produce RA periodically to coordinate the premeiotic transitions, independent of RA from pachytene spermatocytes.

We do not yet know why the pre- and postmeiotic transitions require different cellular sources of RA. In the seminiferous tubule, premeiotic germ cells are confined to the basal compartment, which is separated from the luminal compartment, where pachytene spermatocytes and postmeiotic germ cells are located, by tight junctions formed between Sertoli cells (60) (Fig. 8*B*). This basal vs. luminal arrangement may influence the diffusion, degradation, and availability of RA produced by Sertoli cells and pachytene spermatocytes. However, we surmise that RA is not segregated strictly between basal and luminal compartments. Indeed, in Sertoli cell-specific *Aldh1a1-3*–deficient testes, the resulting arrest at the first (juvenile) spermatogonial differentiation could be rescued by a single injection of RA, with all germ cell layers observed subsequently, in adult testes (28). This suggests that RA from pachytene spermatocytes can diffuse into the basal compartment to affect the two premeiotic transitions, perhaps redundantly with RA from Sertoli cells. Conversely, 20 wk after RA injection, Sertoli cell-specific *Aldh1a1-3*–deficient males displayed abnormalities in release of spermatozoa (28), suggesting that Sertoli cell production of RA may contribute, modestly, to this process. Thus, pachytene spermatocytes may work collaboratively with Sertoli cells to ensure high RA concentrations throughout the seminiferous tubules. Alternatively, the postmeiotic transitions may simply require a higher level of RA (from Sertoli cells plus pachytene spermatocytes) than the premeiotic transitions.

In summary, we conclude that both Sertoli cells and pachytene spermatocytes produce RA to establish a periodicity of testicular RA levels, which coordinate the four key transitions in spermatogenesis in close physical and temporal proximity. Our findings may have practical implications for in vitro spermatogenesis. Recently, successful spermatogenesis from ES cells to haploid spermatid-like cells was achieved by culturing within gonadal aggregates (61). However, postmeiotic spermatogenesis in vitro (to produce functional spermatozoa) has yet to be achieved. Our findings that haploid spermatids require periodic RA signals to complete spermatogenesis may help advance the technology of in vitro gamete production.

## Materials and Methods

**Mice.** Three types of mice were used: WT (C57BL/6NTac), *Dmc1*-deficient (B6.Cg-Dmc1$^{tm1Jcs}$/JcsJ) (50), and *Spo11*-deficient (B6-129X1 Spo11$^{tm1Mjn}$) (52). See *SI Materials and Methods* for strain and genotyping details. Unless otherwise noted, experiments were performed on 6- to 8-wk-old male mice, fed a regular (vitamin A-sufficient) diet. All experiments involving mice were approved by the Committee on Animal Care at the Massachusetts Institute of Technology.

**Statistics.** Unless otherwise noted, data are represented as mean ± SD or SE of three or more biological replicates. When comparing two groups, the *t* test (one-tailed as indicated) was employed. When comparing three or more groups, a one-way ANOVA with the Tukey–Kramer post hoc test was used.

**Histology.** Testes were fixed overnight in Bouin's solution, embedded in paraffin, sectioned, and stained with hematoxylin and periodic acid-Schiff (PAS). All sections were examined using a light microscope. Germ cell types were identified by their location, nuclear size, and chromatin pattern (62). See *SI Materials and Methods* for details on identification of seminiferous tubule stages.

**Chemical Treatments.** Mice received i.p. or s.c. injections of all-*trans* RA, WIN18,446, BrdU, EdU, and/or hydroxyurea (HU). See *SI Materials and Methods* for details.

**Immunostaining on Testis Sections.** Testes were fixed overnight in either Bouin's solution or 4% (wt/vol) paraformaldehyde (PFA), embedded in paraffin, and sectioned at 5 μm thickness. Slides were dewaxed, rehydrated, and heated in 10 mM sodium citrate buffer (pH 6.0). Sections were blocked, incubated with the primary antibody, washed with PBS, and incubated with secondary antibody. Detection was fluorescent or colorimetric. See *SI Materials and Methods* for details.

**Nuclear Spreads of Spermatocytes.** Testes were dissected to obtain single cells, including spermatocytes, as previously described (8). Cell suspensions were placed on slides and fixed in 1% (wt/vol) PFA. Slides were washed, air dried, and stored at −80 °C before use. For immunostaining, slides were brought to room temperature and washed with PBS. See *SI Materials and Methods* for details.

**Single-Molecule Fluorescent in Situ Hybridization.** Probe design, synthesis, and coupling were as previously described (47, 63). Testes were fixed in 4% (wt/vol) PFA and embedded in optimal cutting temperature compound (O.C.T.). Frozen blocks were sectioned at 8 μm thickness and dehydrated overnight in 70% (vol/vol) ethanol at 4 °C. Hybridization was performed as previously described (47, 63). Counting of individual mRNA particles, image stitching, and data analysis were performed using custom Matlab software as previously described (47, 63). See *SI Materials and Methods* for details.

**Absolute Quantification of RA Levels.** Sample preparation and RA quantification were performed according to a published protocol (64). Testes were collected and homogenized by hand in ground glass homogenizers on ice in 1 mL of saline (0.9% NaCl). All-*trans* RA was extracted and quantified by liquid chromatography/mass spectrometry. See *SI Materials and Methods* for details.

**ACKNOWLEDGMENTS.** We thank M. Handel (The Jackson Laboratory) for anti-H1t antisera; M. Kane (University of Maryland) and R. Kang (University of Texas MD Anderson Cancer Center) for helpful suggestions; R. Besada, M. Goodheart, K. Igarashi, T. Kunchok, and Y. Soh for experimental support; and K. Romer, J. Hughes, M. Kojima, M. Mikedis, and P. Nicholls for helpful discussions and critical reading of the manuscript. This work was supported by the Howard Hughes Medical Institute and United States Department of Defense Peer-Reviewed Medical Research Program W81XWH-15-1-0337 (to E.F.).

1. Oakberg EF (1971) Spermatogonial stem-cell renewal in the mouse. *Anat Rec* 169: 515–531.
2. de Rooij DG (1973) Spermatogonial stem cell renewal in the mouse. I. Normal situation. *Cell Tissue Kinet* 6:281–287.
3. Nakagawa T, Nabeshima Y, Yoshida S (2007) Functional identification of the actual and potential stem cell compartments in mouse spermatogenesis. *Dev Cell* 12:195–206.
4. Chan F, et al. (2014) Functional and molecular features of the Id4+ germline stem cell population in mouse testes. *Genes Dev* 28:1351–1362.
5. Shinohara T, Orwig KE, Avarbock MR, Brinster RL (2000) Spermatogonial stem cell enrichment by multiparameter selection of mouse testis cells. *Proc Natl Acad Sci USA* 97:8346–8351.
6. Monesi V (1962) Autoradiographic study of DNA synthesis and the cell cycle in spermatogonia and spermatocytes of mouse testis using tritiated thymidine. *J Cell Biol* 14:1–18.
7. Baltus AE, et al. (2006) In germ cells of mouse embryonic ovaries, the decision to enter meiosis precedes premeiotic DNA replication. *Nat Genet* 38:1430–1434.
8. Anderson EL, et al. (2008) Stra8 and its inducer, retinoic acid, regulate meiotic initiation in both spermatogenesis and oogenesis in mice. *Proc Natl Acad Sci USA* 105:14976–14980.
9. Oakberg EF (1956) Duration of spermatogenesis in the mouse and timing of stages of the cycle of the seminiferous epithelium. *Am J Anat* 99:507–516.
10. Oakberg EF (1956) A description of spermiogenesis in the mouse and its use in analysis of the cycle of the seminiferous epithelium and germ cell renewal. *Am J Anat* 99:391–413.
11. de Rooij DG (2001) Proliferation and differentiation of spermatogonial stem cells. *Reproduction* 121:347–354.
12. Muciaccia B, et al. (2013) Novel stage classification of human spermatogenesis based on acrosome development. *Biol Reprod* 89:60.
13. Huckins C (1971) The spermatogonial stem cell population in adult rats. I. Their morphology, proliferation and maturation. *Anat Rec* 169:533–557.
14. Leblond CP, Clermont Y (1952) Spermiogenesis of rat, mouse, hamster and guinea pig as revealed by the periodic acid-fuchsin sulfurous acid technique. *Am J Anat* 90: 167–215.
15. Lok D, Weenk D, De Rooij DG (1982) Morphology, proliferation, and differentiation of undifferentiated spermatogonia in the Chinese hamster and the ram. *Anat Rec* 203:83–99.
16. Sylvester SR, Griswold MD (1994) The testicular iron shuttle: A "nurse" function of the Sertoli cells. *J Androl* 15:381–385.
17. van Pelt AM, de Rooij DG (1990) Synchronization of the seminiferous epithelium after vitamin A replacement in vitamin A-deficient mice. *Biol Reprod* 43:363–367.
18. Van Pelt AM, De Rooij DG (1990) The origin of the synchronization of the seminiferous epithelium in vitamin A-deficient rats after vitamin A replacement. *Biol Reprod* 42:677–682.
19. van Pelt AM, de Rooij DG (1991) Retinoic acid is able to reinitiate spermatogenesis in vitamin A-deficient rats and high replicate doses support the full development of spermatogenic cells. *Endocrinology* 128:697–704.
20. Oulad-Abdelghani M, et al. (1996) Characterization of a premeiotic germ cell-specific cytoplasmic protein encoded by Stra8, a novel retinoic acid-responsive gene. *J Cell Biol* 135:469–477.
21. Zhou Q, et al. (2008) Expression of stimulated by retinoic acid gene 8 (Stra8) in spermatogenic cells induced by retinoic acid: An in vivo study in vitamin A-sufficient postnatal murine testes. *Biol Reprod* 79:35–42.
22. Endo T, et al. (2015) Periodic retinoic acid-STRA8 signaling intersects with periodic germ-cell competencies to regulate spermatogenesis. *Proc Natl Acad Sci USA* 112:E2347–E2356.
23. Chung SS, Sung W, Wang X, Wolgemuth DJ (2004) Retinoic acid receptor alpha is required for synchronization of spermatogenic cycles and its absence results in progressive breakdown of the spermatogenic process. *Dev Dyn* 230:754–766.
24. Chung SSW, Wang X, Wolgemuth DJ (2005) Male sterility in mice lacking retinoic acid receptor alpha involves specific abnormalities in spermiogenesis. *Differentiation* 73:188–198.
25. Chung SS, Wang X, Wolgemuth DJ (2009) Expression of retinoic acid receptor alpha in the germline is essential for proper cellular association and spermiogenesis during spermatogenesis. *Development* 136:2091–2100.
26. Chung SS, et al. (2011) Oral administration of a retinoic Acid receptor antagonist reversibly inhibits spermatogenesis in mice. *Endocrinology* 152:2492–2502.
27. Hasegawa K, Saga Y (2012) Retinoic acid signaling in Sertoli cells regulates organization of the blood-testis barrier through cyclical changes in gene expression. *Development* 139:4347–4355.
28. Raverdeau M, et al. (2012) Retinoic acid induces Sertoli cell paracrine signals for spermatogonia differentiation but cell autonomously drives spermatocyte meiosis. *Proc Natl Acad Sci USA* 109:16582–16587.
29. Chung SS, Wang X, Wolgemuth DJ (2016) Prolonged oral administration of a pan-retinoic acid receptor antagonist inhibits spermatogenesis in mice with a rapid recovery and changes in the expression of influx and efflux transporters. *Endocrinology* 157:1601–1612.
30. Hogarth CA, et al. (2011) Suppression of Stra8 expression in the mouse gonad by WIN 18,446. *Biol Reprod* 84:957–965.
31. Bowles J, et al. (2006) Retinoid signaling determines germ cell fate in mice. *Science* 312:596–600.
32. Koubova J, et al. (2006) Retinoic acid regulates sex-specific timing of meiotic initiation in mice. *Proc Natl Acad Sci USA* 103:2474–2479.
33. Kluin PM, Kramer MF, de Rooij DG (1982) Spermatogenesis in the immature mouse proceeds faster than in the adult. *Int J Androl* 5:282–294.
34. Ghyselinck NB, et al. (2006) Retinoids and spermatogenesis: Lessons from mutant mice lacking the plasma retinol binding protein. *Dev Dyn* 235:1608–1622.
35. Ashley T, Gaeth AP, Creemers LB, Hack AM, de Rooij DG (2004) Correlation of meiotic events in testis sections and microspreads of mouse spermatocytes relative to the mid-pachytene checkpoint. *Chromosoma* 113:126–136.
36. Mahadevaiah SK, et al. (2001) Recombinational DNA double-strand breaks in mice precede synapsis. *Nat Genet* 27:271–276.
37. Yuan L, et al. (2000) The murine SCP3 gene is required for synaptonemal complex assembly, chromosome synapsis, and male fertility. *Mol Cell* 5:73–83.
38. Drabent B, Bode C, Bramlage B, Doenecke D (1996) Expression of the mouse testicular histone gene H1t during spermatogenesis. *Histochem Cell Biol* 106:247–251.
39. Turner JM, et al. (2004) BRCA1, histone H2AX phosphorylation, and male meiotic sex chromosome inactivation. *Curr Biol* 14:2135–2142.
40. Snyder EM, Small C, Griswold MD (2010) Retinoic acid availability drives the asynchronous initiation of spermatogonial differentiation in the mouse. *Biol Reprod* 83:783–790.
41. Hogarth CA, et al. (2013) Turning a spermatogenic wave into a tsunami: Synchronizing murine spermatogenesis using WIN 18,446. *Biol Reprod* 88:40.
42. Vernet N, et al. (2006) Retinoic acid metabolism and signaling pathways in the adult and developing mouse testis. *Endocrinology* 147:96–110.
43. Sugimoto R, Nabeshima Y, Yoshida S (2012) Retinoic acid metabolism links the periodical differentiation of germ cells with the cycle of Sertoli cells in mouse seminiferous epithelium. *Mech Dev* 128:610–624.
44. Koç A, Wheeler LJ, Mathews CK, Merrill GF (2004) Hydroxyurea arrests DNA replication by a mechanism that preserves basal dNTP pools. *J Biol Chem* 279:223–230.
45. Platt OS (2008) Hydroxyurea for the treatment of sickle cell anemia. *N Engl J Med* 358: 1362–1369.
46. Oud JL, de Jong JH, de Rooij DG (1979) A sequential analysis of meiosis in the male mouse using a restricted spermatocyte population obtained by a hydroxyurea/triaziquone treatment. *Chromosoma* 71:237–248.
47. Raj A, van den Bogaard P, Rifkin SA, van Oudenaarden A, Tyagi S (2008) Imaging individual mRNA molecules using multiple singly labeled probes. *Nat Methods* 5:877–879.
48. Matt N, et al. (2005) Retinoic acid-dependent eye morphogenesis is orchestrated by neural crest cells. *Development* 132:4789–4800.
49. Bowles J, et al. (2016) ALDH1A1 provides a source of meiosis-inducing retinoic acid in mouse fetal ovaries. *Nat Commun* 7:10845.
50. Pittman DL, et al. (1998) Meiotic prophase arrest with failure of chromosome synapsis in mice deficient for *Dmc1*, a germline-specific RecA homolog. *Mol Cell* 1:697–705.
51. Yoshida K, et al. (1998) The mouse RecA-like gene Dmc1 is required for homologous chromosome synapsis during meiosis. *Mol Cell* 1:707–718.
52. Baudat F, Manova K, Yuen JP, Jasin M, Keeney S (2000) Chromosome synapsis defects and sexually dimorphic meiotic progression in mice lacking Spo11. *Mol Cell* 6:989–998.
53. Romanienko PJ, Camerini-Otero RD (2000) The mouse Spo11 gene is required for meiotic chromosome synapsis. *Mol Cell* 6:975–987.
54. Tokuda M, Kadokawa Y, Kurahashi H, Marunouchi T (2007) CDH1 is a specific marker for undifferentiated spermatogonia in mouse testes. *Biol Reprod* 76:130–141.
55. Chambon P (1996) A decade of molecular biology of retinoic acid receptors. *FASEB J* 10:940–954.
56. Hosken DJ, Hodgson DJ (2014) Why do sperm carry RNA? Relatedness, conflict, and control. *Trends Ecol Evol* 29:451–455.
57. Hogarth CA, et al. (2015) Processive pulses of retinoic acid propel asynchronous and continuous murine sperm production. *Biol Reprod* 92:37.
58. Snyder EM, Davis JC, Zhou Q, Evanoff R, Griswold MD (2011) Exposure to retinoic acid in the neonatal but not adult mouse results in synchronous spermatogenesis. *Biol Reprod* 84:886–893.
59. Timmons PM, Rigby PW, Poirier F (2002) The murine seminiferous epithelial cycle is pre-figured in the Sertoli cells of the embryonic testis. *Development* 129:635–647.
60. Mruk DD, Cheng CY (2004) Sertoli-Sertoli and Sertoli-germ cell interactions and their significance in germ cell movement in the seminiferous epithelium during spermatogenesis. *Endocr Rev* 25:747–806.
61. Zhou Q, et al. (2016) Complete meiosis from embryonic stem cell-derived germ cells in vitro. *Cell Stem Cell* 18:330–340.
62. Russell LD, Ettlin RA, Sinha Hikim AP, Clegg ED (1990) *Histological and Histopathological Evaluation of the Testis* (Cache River Press, Clearwater, FL).
63. Peterson KA, et al. (2012) Neural-specific Sox2 input and differential Gli-binding affinity provide context and positional information in Shh-directed neural patterning. *Genes Dev* 26:2802–2816.
64. Kane MA, Napoli JL (2010) Quantification of endogenous retinoids. *Methods Mol Biol* 652:1–54.
65. Soh YQ, et al. (2015) A gene regulatory program for meiotic prophase in the fetal ovary. *PLoS Genet* 11:e1005531.
66. Amory JK, et al. (2011) Suppression of spermatogenesis by bisdichloroacetyldiamines is mediated by inhibition of testicular retinoic acid biosynthesis. *J Androl* 32:111–119.
67. Cobb J, Cargile B, Handel MA (1999) Acquisition of competence to condense metaphase I chromosomes during spermatogenesis. *Dev Biol* 205:49–64.
68. Bellani MA, Romanienko PJ, Cairatti DA, Camerini-Otero RD (2005) SPO11 is required for sex-body formation, and Spo11 heterozygosity rescues the prophase arrest of Atm-/- spermatocytes. *J Cell Sci* 118:3233–3245.
69. Kluin PM, Kramer MF, de Rooij DG (1984) Proliferation of spermatogonia and Sertoli cells in maturing mice. *Anat Embryol (Berl)* 169:73–78.
70. Vergouwen RP, Jacobs SG, Huiskamp R, Davids JA, de Rooij DG (1991) Proliferative activity of gonocytes, Sertoli cells and interstitial cells during testicular development in mice. *J Reprod Fertil* 93:233–243.
71. Lok D, de Rooij DG (1983) Spermatogonial multiplication in the Chinese hamster. III. Labelling indices of undifferentiated spermatogonia throughout the cycle of the seminiferous epithelium. *Cell Tissue Kinet* 16:31–40.
72. Huckins C (1971) The spermatogonial stem cell population in adult rats. II. A radioautographic analysis of their cell cycle properties. *Cell Tissue Kinet* 4:313–334.
73. Lok D, Jansen MT, de Rooij DG (1983) Spermatogonial multiplication in the Chinese hamster. II. Cell cycle properties of undifferentiated spermatogonia. *Cell Tissue Kinet* 16:19–29.
74. Kotaja N, Sassone-Corsi P (2007) The chromatoid body: A germ-cell-specific RNA-processing centre. *Nat Rev Mol Cell Biol* 8:85–90.
75. Niederreither K, Fraulob V, Garnier JM, Chambon P, Dollé P (2002) Differential expression of retinoic acid-synthesizing (RALDH) enzymes during fetal development and organ differentiation in the mouse. *Mech Dev* 110:165–171.